

# Impact of Photovoltaic Oriented DC Stray Current Corrosion on Large Scale Solar Farms' Grounding and Third-Party Infrastructure: Modelling and Assessment

Charalambos A.  
Charalambous

Member, IEEE  
Power System Modelling (PSM)  
Laboratory  
University of Cyprus  
PO BOX 20537  
Nicosia, TT134, 1678, Cyprus  
cchara@ucy.ac.cy

Andreas Dimitriou

Power System Modelling (PSM)  
Laboratory  
University of Cyprus  
PO BOX 20537  
Nicosia, TT134, 1678, Cyprus

Nikolaos Kokkinos

Member, IEEE  
ELEMKO, SA  
90 TATOIOU  
Metamorphosis, 144 52, Greece  
n.kokkinos@elemko.gr

**Abstract** – This paper discusses the impact of Photovoltaic oriented DC stray current corrosion on large scale solar farms' grounding and third-party infrastructure. The DC stray current may result from a fault or facilitated by buried cables' condition that allows DC leakage to flow into the earth. In particular, such abnormal conditions can impact the grounding electrodes of the PV plants as well as third-party metallic infrastructures (e.g. natural gas pipelines) that are laid in the nearby vicinity of a solar plant. The paper unfolds by thoroughly addressing three specific objectives: a) defining the origin of the problem, b) modelling the problem in commercially available software and c) discussing the arising implications.

**Index Terms** — Solar Systems, DC Stray Current, Corrosion, Grounding electrodes, Metallic pipelines.

## I. INTRODUCTION

The development of large scale photovoltaic (PV) plants in rural and industrial areas is relentlessly increasing, as this type of plants play an integral role in the promotion of distributed energy generation from renewable sources [1], [2]. To this extent, an important pylon for safely dispatching solar energy rests with installing appropriate grounding systems that would limit the impact on personnel, from the perspective of touch and step voltages/currents and corrosion [3]-[4]. In particular, an adequate grounding system is fundamental for effective lightning and surge protection endeavours applied in large scale PV plants [5]-[6].

Nonetheless, an important issue that has received less attention rests with misinterpreting existing approved grounding methods, which thus far are not directly related to large PV systems (NB: the CENELEC document of TS 50539-11: 2010 [7] only describes the application principles for grounding and surge protection in small PV installations on roofs of domestic structures).

Thus, the arising misinterpretations may lead to failures in the field pertaining to loss of mechanical integrity e.g. module frames, grounding installation errors and damage from corrosion to grounding and supporting/foundation infrastructure of the PV modules. To a large extent,

contractors are following installation recommendations regarding the use of proper materials and components and they are avoiding connections of dissimilar metals that may lead to galvanic corrosion. Galvanic corrosion is a process by which two metals can electrochemically corrode when in contact with an electrolyte. If not mitigated, this corrosion can lead to extremely dangerous and costly failures in fixtures and fittings of the plant such as in PV façade-frameworks [8]. Consequently, an important parameter that contractors take into account when selecting the ground electrode material is the foundation type that interfaces the PV façade- framework to the ground electrode system [9].

Although the potential problems arising from galvanic corrosion are known to the PV installation industry, the corrosion impact of DC stray current originating from the operation or maloperation of large scale PV plants remains unexplored. Stray current corrosion refers to corrosion damage resulting from current flow other than in the intended circuit (e.g. flowing through soil.)

To this end, this paper lists as the first attempt in the archived literature to approach the impact of Photovoltaic oriented DC stray current corrosion on large scale solar farms' grounding and nearby third-party infrastructure. It unfolds by holistically addressing three specific objectives: a) defining the origin of the problem, b) modelling the problem in commercially available software and c) discussing the arising implications.

## II. DEFINITION OF THE PROBLEM

### A. DC Leakage Currents from PV Systems

A PV plant has a distinct potential against ground. Thus, sufficient insulation is required to prevent current from the PV plant leaking to ground. The total ground current, also known as leakage current, is formed by the contribution of all system components (e.g. PV modules, DC cables, Inverters) when taken together. For a certain voltage level, this leakage current decodes into an effective insulation resistance that is known as  $R_{ISO}$  (see Fig. 1).

The effective insulation resistance  $R_{ISO}$  is measured [10] before connecting the PV system to the grid and it provides an indication of the magnitude of the anticipated leakage currents to ground. The insulation resistance ( $R_{ISO}$ ) of the entire system (all PV modules, DC circuitry, supporting infrastructure and inverter) is monitored by the inverter.

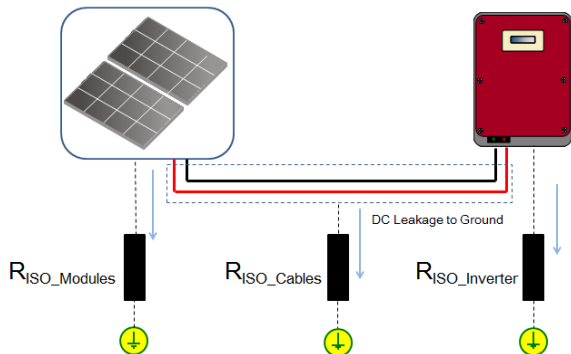


Fig. 1. Effective Insulation Resistance ( $R_{ISO}$ ) Decomposed in Constituent Elements

Moreover, the standard industrial practice suggests that PV strings are designed for the highest DC voltage to reduce  $I^2R$  losses. However, in large scale applications, multiple strings are located in parallel, thus raising the current. The arrangement in multiple strings entails a large geographic distribution of the DC wirings. Hence, three characteristics of a PV system design that enable DC leakage activity and perhaps DC arc fault risks are: a) the high DC voltage, b) the high DC current and c) the large geographic distribution of the DC circuitry.

Primarily in PV systems, it is possible to have leakage current to frames emanating from the PV modules. This is an inevitable phenomenon comprising very minor amounts of current leaking from the cells to the module frames. This leakage current typically occurs via the module glass. If the system grounded, the leakage current moves from the frame to ground circuit and returns via the grounded polarity conductor to the modules. Moreover, in both grounded and floating PV systems (have neither the positive nor negative DC wires connected to earth), the leakage current emanating from their DC wiring system may reach underground metallic structures. This is because, the DC wiring in large PV plants is geographically distributed (this can be estimated at 2.5 km in a 1MW PV plant) within soil, thus forbidding its visual inspection. Thus, if the insulation of buried DC wires becomes ineffective or deteriorated - due to moisture ingress, freeze/thaw cycles or accidental damages will lead to increased leakage fault currents through the soil and/or through buried conductor before returning back to the energy source. Thus, the leakage activity in PV systems is likely to be dominated by the condition of the buried DC circuitry.

The leakage currents will increase in wet weather/soil conditions, with PV system size and as the system ages or in the event of DC ground faults. A ground fault in a floating system, that falls below the detection level of Ground Fault Protective Devices, is usually realized through impedance measurements (between array conductors and ground). It may

be also monitored as a loss of power in the system, if the data monitoring systems have adequate sensitivity.

### B. Stray Current Mechanism and Impact on Grounding Electrodes and Third party Infrastructure

As detailed above, paradigms of DC stray/leakage current originating from the operation or maloperation of large scale PV plants include ground faults such as live DC circuit connection to frames, or leakage current originating from buried PV DC cables with low or faulty/deteriorated insulation. The steady flow of DC current into the earth, can last from a few minutes to several days/months. This current is subsequently picked up on nearby underground metallic structures (e.g. gas pipelines) and may travel for a considerable distance before discharging. Severe damage can occur on the metallic structures at the current discharge location. Even a small leakage current if let unattended, or hidden in the background, may cause accelerated stray current corrosion on a metallic underground infrastructure lying in the area [11].

The mechanism of stray current corrosion in large-scale PV applications can be explicitly described as follows: The leakage current (vastly from buried DC cables) will flow in to the ground and subsequently flow along parallel circuits either directly through the soil and/or through buried conductor before returning back to the energy source. Therefore a current loop is formed through the soil and/or the grounding electrodes/ nearby metallic structures. Thus, both the system grounding as well as any nearby metallic structures provide a path for ground-fault leakage currents to return to the energy source. Given that current flow in a metallic conductor is electronic, while that through electrolytes such as the soil, concrete, etc., is ionic, it follows that there must be an electron to ion transfer as current leaves a metallic conductor to earth. Therefore, where a current leaves metallic-pathways to earth (i.e. to return to the energy source) there will, therefore, be an oxidation, or electron-producing, reaction. This reaction is visible after time as corrosion damage. Corrosion of metallic objects will, therefore, occur from each point that current transfers from a metallic conductor to an electrolyte.

Therefore, in the context of large scale PV systems, DC stray current corrosion may have an immense impact on the grounding electrodes and the metal foundation of the PV plant supporting infrastructure as well as on any third party infrastructure (e.g. natural gas pipelines) that rests in the nearby vicinity (See Fig. 2). It must be noted that the concept shown in Fig.2 is merely illustrative and the direction of stray current flow indicated by the arrows is a simplistic illustration.

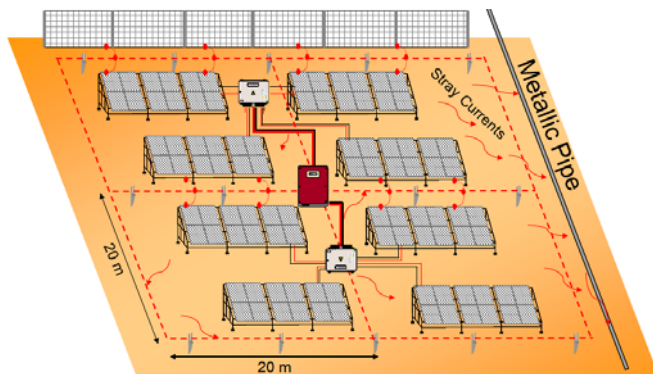


Fig. 2. Stray DC Leakage Currents from PV System Reaching a Metallic Pipe through Soil

### III. DESCRIPTION OF PHYSICAL MODEL

#### A. Layout and Electrical Specifications

Figure 3 illustrates a topologically-accurate top-view of a floating PV system. It labels its actual dimensions as well as the most important features identified as crucial when it comes to assessing the stray current corrosion impact from a PV system operation. This physical model has been chosen as an example system that can be replicated in a simulation platform (see Section IV).

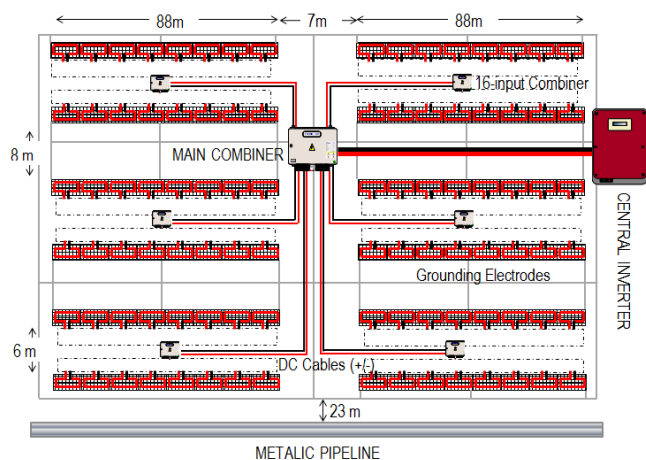


Fig. 3. Top-View of a Realistic PV Park with Actual Dimensions Labelling its Elemental Components

In particular, the PV system considered has a nominal output power of 528kWp and can be directly linked to the MV network. It is occupying an area of 7875.2 m<sup>2</sup> which hosts twelve similar structures (arrays) of fixed inclination. The PV modules are collectively wired in series strings e.g. the positive lead wire of one module is connected to the negative lead wire of the next module. This results in a cumulative voltage output without altering the current. Thus for example, two series strings imply two sets of wires, two positives and two negatives. The output wires from multiple series strings (positive and negatives) are subsequently joined in combiner boxes. From the combiners the wires are directed to a central combiner and from thereon to a central inverter.

For clarity, Fig. 3 illustrates only the wires (positive and negative) from each combiner to the central combiner and the wires routed from the central combiner to the central inverter.

More explicitly, in the system considered the PV modules (each 250W) are configured in 22-modules strings with 16 source circuits per combiner box. At standard test conditions (1000 W/m<sup>2</sup>) each 250 W module has an  $I_{mp}$  of 8.1 A and hence the  $I_{mp}$  of the PV output circuit per combiner box is 129.6 A. Each module's  $I_{sc}$  is 8.67 A and the  $I_{sc}$  of the output PV circuit per combiner box is 142.56 A. Working voltages are for a 250 W module  $V_{mp}$  30.94 V and for each 22-module string  $V_{mp}$  is 680.68 V.

#### B. DC Cables Specification

The standard industrial practice suggests that combiners are used to eliminate running multiple DC wires from the PV arrays to the inverter as a means to reduce wiring costs and possibly installation costs. The current carrying requirements of the wires leading to central inverters are increased, since these should conduct the combined amount of currents coming from multiple PV strings. Thus, PV designers are thoroughly assessing the optimal size of dc wires (by virtue of their duty), especially those that run from combiner boxes to the location of the inverters. The assessment largely pertains in avoiding the increase of conductors' power losses since these losses may erode the percentage of the potential solar energy harvest. However, if the conductors are over-specified to minimize the power losses, the overall system costs will escalate and unavoidably the levelized cost of solar energy will rise.

To this end, the manufacturers of DC cables suitable for PV installations specify a range of technical characteristics, which include: a) electrical parameters (e.g. rated voltage, ampacity, max. permissible DC voltage, etc.), b) thermal parameters (e.g. ambient temperatures, max. permissible conductor operating temperature, short-circuit temperature etc.), c) mechanical parameters (e.g. tensile rating, min. bending radius etc.) and d) chemical parameters (e.g. acid and alkaline resistance, ammonia resistance, environmental condition resistance). It should be highlighted that those PV DC cables that are directly buried into the ground may follow some installation guidelines such the ones given for example in VDE 0800 Section 174 § 5.4.2 and VDE 0891 Section 6 § 4.2 ratings.

#### C. Grounding System Description

The use of type B electrodes (that ensure the equipotential bonding of all PV metal frames-works) is assumed to be the case in the example PV system shown in Fig. 3. For type B grounding electrodes the most common shape used is the strip conductor. To achieve an effective grounding system, the strip conductor is usually installed into the soil within a trench of about 0,5m deep and 0,5m wide, using some sort of fasteners.

#### D. Metallic Infrastructure Buried in Nearby Vicinity

It is quite common for large PV plants installed in rural areas to be near metallic infrastructures, such as buried gas/oil pipelines or irrigation pipelines. Thus, a sufficiently-

sized, buried metallic pipeline exists near the PV system as illustrated in Figs. 2 and 3.

#### IV. SIMULATION MODEL AND PARAMETERS

A simulation model is developed following an assessment of the infrastructure elements considered likely to be affected from leakage current originating from floating buried PV DC cables with low or faulty/deteriorated insulation. The simulation platform used [12] allows currents to be injected and collected at various points in a network of conductors which are placed in a soil environment. Subject to users' intervention, the simulation platform is able to further compute the flow of these currents through each individual conductor within the network modelled. It thus allows computing a stray current and a voltage distribution along the actual length of the entire system of conductors considered. The computer model formulated to replicate the physical configuration shown in Fig. 3 is illustrated in perspective view in Fig.4. This model allows for the stray current performance of the PV plant's grounding and nearby infrastructure to be assessed in terms of their geometry, topological arrangement as well as soil and material characteristics.

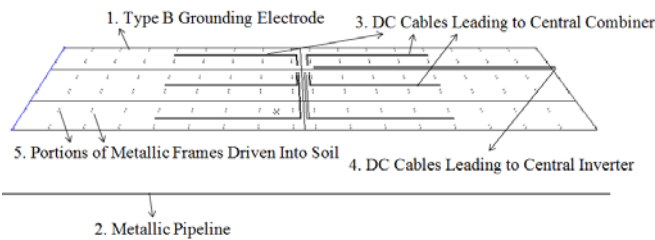


Fig. 4. Perspective view of the arrangement of conductive elements in the PV System Model

##### A. Description of Conductors' Sizing and Arrangement

With reference to Fig.4 the numbered items are described in more detail:

###### 1) Type B - Grounding Electrode

Due to software constraints, the type B grounding electrodes are modelled as cylindrical conductors, buried at some distance below the earth surface. The radius of the cylindrical conductors are given a radius of 5.35 mm, to provide an equivalent per unit length volume as that of a strip conductor with dimensions 30mm x 3mm.

###### 2) Metallic Pipeline

The conductor representing the metallic pipeline serves the scope of assessing the effect of stray currents on samples of the metallic infrastructure that may be present in the nearby vicinity of the PV Park. Within the model developed it takes the form of a hollow coated conductor, which may be located at a range of distances from the PV system.

###### 3) DC Cables Leading to Central Combiner

In PV systems, both the positive and negative cable conductors are current-carrying. Therefore the size of the floating cable conductors (positive and negative) is based on their required ampacity value. The minimum required

ampacity of these cables can be determined from the  $I_{sc}$  of the output PV circuit per combiner box and a de-rating multiplier as per the directives given in USA National Electrical Code (NEC), 2008. Thus, the size of the DC cables in the model is selected as per Table 310.16 of the 2008 NEC. Moreover, each conductor is coated with a PVC layer of sufficient thickness to provide the specified insulation resistance of the cable in  $M\Omega.km$ . The conductors are buried into a soil model, 0.25m below the earth surface.

###### 4) DC Cables Leading to Central Combiner

A similar process to the one described above is followed for the cables leading to the central inverter. However, the minimum required ampacity of these floating cables is determined from the  $I_{sc}$  of the combined output PV circuit from each combiner box and a de-rating multiplier as per 2008 NEC. Moreover an adequately sized PVC layer is calculated to provide the specified insulation resistance of the cable in  $M\Omega.km$ . These conductors are also assumed to be laid in a soil model, 0.25m below the earth surface.

###### 5) Portions of Metallic Frames Driven to Soil.

These are galvanized steel conductors that are modelled to replicate the portions of the PV façade- frameworks driven into the soil. These portions are interfaced to the grounding electrode system to ensure the equipotential bonding of all PV metal frames-works/grounding electrodes.

##### B. Base Input Data and Assumptions

Table I tabulates the base input data and assumptions for the items 1 -5 shown in Fig.4. These are employed in the simulation for assessing the stray current performance of the of the PV system model.

TABLE I  
BASE INPUT DATA AND ASSUMPTIONS

	Element Description	Parameter Description
1	Type B - Grounding Electrode	Total Length of Grounding Electrode: 864.4m Buried Depth: 0.5 m Conductor Material: Copper Conductor CSA: 89.9 mm <sup>2</sup>
2	Metallic Pipeline	Total Length Modelled: 210 m Location: 23m away from the northern side of the PV Park (parallel routing) Pipeline Material: Heavy Duty Galvanized Steel. Pipeline Size: Internal Radius 0.17m, External Radius: 0.20m Coating Material/Thickness: Lead (Pb)/ 5mm.
3	DC Cables Leading to Central Combiner	Length of all Cables Modelled: 683.6m Buried Depth: 0.25m Conductor Material: Copper Conductor CSA: 54mm <sup>2</sup> Coating Material/thickness: PVC /5mm Coating Resistivity: 6.38*10 <sup>11</sup> Ω.m Effective Insulation Resistance to Earth: 25.14 MΩ.km
4	DC Cables Leading to Central Inverter	Length of all Cables Modelled: 175m Buried Depth: 0.25m Conductor Material: Copper Conductor CSA: 1013 mm <sup>2</sup> Coating Material/thickness: PVC /8mm Coating Resistivity: 6.38*10 <sup>11</sup> Ω.m Effective Insulation Resistance to Earth: 26.23MΩ.km
5	Portions of Metallic Frames Driven into the Soil	Length of each portion driven into the soil: 0.8m Number of elements (portions) modelled in the system: 216 Material: Galvanized Steel Effective CSA of each portion: 141mm <sup>2</sup>

### C. Description of Soil Model

The simulation model shown in Fig.4 incorporates a uniform soil model that is embedded in the software platform used [13]. The resistivity assigned to the model can take a range of values depending on the soil type and moisture content (e.g. 10  $\Omega$ .m 100  $\Omega$ .m etc.).

### D. Description of Energisation Principles

The model is discretely energized through all DC conductor cables present in the simulation model of Fig. 4. The concept of energisation, on an individual set of cables (positive and negative), is illustrated in Fig. 5. The energisation is achieved by the use of current sources and sinks. This is an artificial component of the software used that allows an indirect snapshot of the DC circuitry's static power flow.

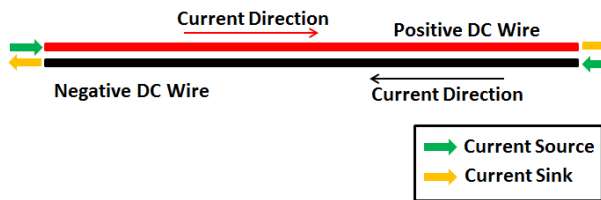


Fig. 5. Current Energisation Principle applied on a Set of DC Cables

In particular, the simulation model in Fig. 4 embraces the following set of cables (positive and negative): a) cables from each combiner box to the central combiner and b) cables routed from the central combiner to the central inverter, as per the topology of the physical model shown in Fig. 3. There exist 6 combiner boxes and from each box, a set of positive and negative cables are routed to the central combiner. Two more cables are routed to the central inverter; therefore the total number of cables present in the simulation model is 14. Each cable's end is attached to a current source and a current sink respectively. To make the concept more explicit for a floating PV system, if for example a current of +700 A is injected in one end of the cable (e.g. at the location of the central combiner), the same current (-700 A) should be drawn at the other end of the cable (e.g. at the location of the central inverter). Thus, the direction of current in each cable is accordingly specified. It is therefore ensured that the current direction in a positive cable has the opposite direction to its pair negative cable. Table II summarises the  $I_{mp}$  and  $I_{sc}$  output current of each type of cables considered.

TABLE II  
BASE INPUT DATA AND ASSUMPTIONS

	$I_{mp}$	$I_{sc}$
Twelve DC Cables Leading to the Central Combiner (six positive & six negative)	129.6 A	142.56 A
Two DC Cables Leading to the Central Inverter (one positive & one negative)	777.6 A	855.36 A

## V. SIMULATION RESULTS AND ANALYSIS

The simulations are carried out using the PV system illustrated in Fig. 4 under the parameters described in Table I.

The simulation of a static model takes about 20 seconds to be completed on a standard computer (2GHz processor, 3GB RAM).

### A. Simulation of a Static Model

The static model is initially simulated under the rated  $I_{sc}$  of the output PV circuit of each combiner box (i.e. 142.56 A) and the rated  $I_{sc}$  of the output PV circuit leading to the inverter (i.e. 855.36 A), using the energisation principles described in Section IV-D. This represents a worse static scenario in terms of the maximum current that each cable is rated to carry. However, this particular static model assumes that the DC cables' insulation is new, clean and dry (i.e. just after the installation process - e.g. as per the data described in Table I). Therefore, no significant leakage activity should be anticipated.

Nonetheless, Fig. 6 illustrates both the simulated cable to earth voltage and the stray current profile of the positive DC cable leading to the central inverter. The rated  $I_{sc}$  (855.36 A) flows through the cable and therefore produces a rise in the cable to earth potential which in turn results in stray currents. In a floating system, under the rated  $I_{sc}$  the voltage will appear on the cable as +600 mV to remote earth near the central combiner (i.e. injection point) and -600 mV to remote earth near the inverter (i.e. collection point). At midpoint down the cable, the voltage to remote earth will be 0 V. Thus, the total stray current leaving the cable system is determined by the resistance of the cable insulation material and the voltage to earth profile of the cable.

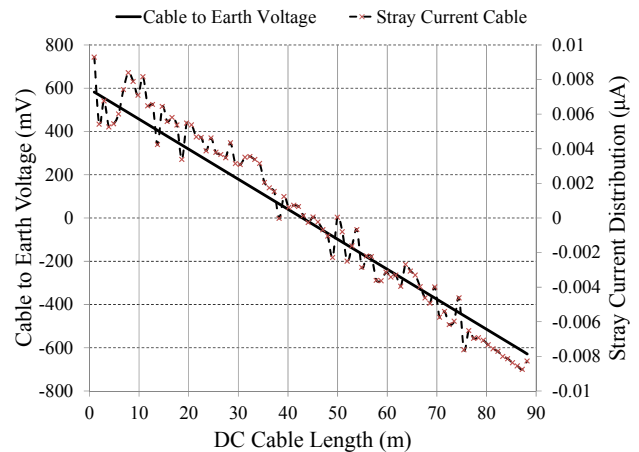


Fig. 6. Cable to Earth Voltage and Associated Stray Current Profile (DC Cable leading to Central Inverter) -- for the specific system modelled

Table III illustrates a summary of the total (calculated) stray current leaving all DC cables considered in the system. The total stray current refers to the sum of all positive leakage currents calculated along each of the cable's length.

TABLE III  
CUMULATIVE STRAY CURRENT LEAVING THE CABLES

Description	Total Cable Length (m)	Stray Current ( $\mu\text{A}$ )
Total Stray Current from DC Cables Leading to the Central Combiner	683.6m	5.55e-03
Total Stray Current from DC Cables Leading to the Central Inverter	175 m	3.09e-03

Moreover, Fig. 7 illustrates the static stray current activity simulated along the length of one of the horizontal grounding electrodes that sits closer to the metallic pipeline (see Fig. 4).

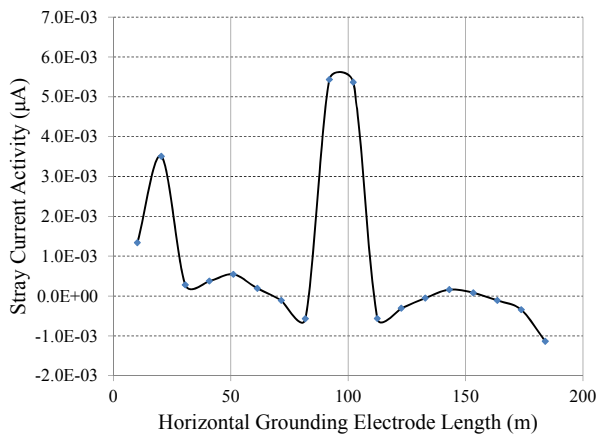


Fig. 7. Stray Current Activity on a Horizontal Grounding Electrode. – for the specific system modelled

The simulated activity shows how the stray current picked up by the horizontal grounding electrode, discharges to earth. This is, in fact, indicated by the positive current values in the simulated profile. A positive value implies that the current is leaking out of the grounding electrode by corrosion. The negative current values imply that some current is leaking back into the grounding electrode. The simulated activity has also shown some localized high stray current activity e.g. at 100 m. This is attributed to the relative positioning between the DC cables (which act as the source of stray currents) and the horizontal grounding electrode under assessment. This implies that some sections of the grounding electrodes (near the source of stray/leakage current) will be more influenced.

To this extent, a different profile is observed when simulating the stray current activity of the buried metallic pipeline. This is clearly shown in Fig. 8. In this case, a localized high stray current activity is observed near 150m, reflecting on its different position relative to the stray current sources (i.e. buried DC cables).

Nevertheless, both responses (Fig. 7 and Fig.8) evidently show the ability of the developed model to examine localized stray current distributions on grounding and third party infrastructures associated with the PV Park.

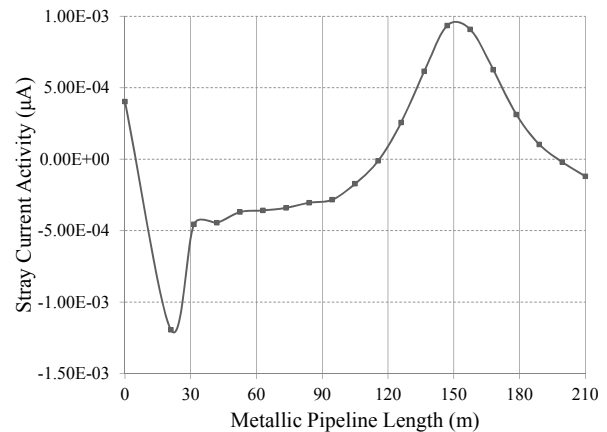


Fig. 8. Stray Current Activity on the Metallic Pipeline – for the specific system modelled

### B. Quantifying the Annual Impact of Stray Current Corrosion on Metallic Infrastructure

#### 1) General Assumptions and Statistical Approach

To quantify the annual impact of stray current corrosion on the metallic infrastructure associated with a PV plant (e.g. grounding electrodes, metallic pipeline etc.) the following norms should be specified:

- *Norm 1:* The level of DC stray current originating from underground DC cables would be proportional to the intrinsic generation characteristics of the PV system.
- *Norm 2:* The level DC stray current flowing through the soil is likely to be affected by the seasonal variations in soil resistivity over a year.

Thus, the above two norms should be used for determining some leveled “seasonal” values of current flow through the system’s underground DC cables. To compute the seasonal leveled figures, a set of dc current measurements were obtained [14] from an operational PV system. The measurements were obtained on a 15minute interval over a complete year. They specifically pertain to a mono-crystalline PV system located in a region with an annual solar potential of approximately 2000 kWh/m<sup>2</sup>. Figure 9, in particular, illustrates a three day summer profile of the measured positive dc current produced by this particular mono-crystalline PV system.

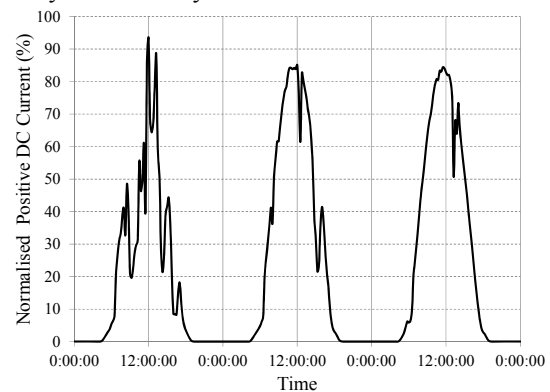


Fig. 9. Normalized Positive DC Current Measurements (Three Day Summer Profile).

The measured values shown in Fig. 9 are normalized over the rated  $I_{sc}$  of the DC cables serving the particular application. The first feature that can be extracted from Fig. 9 relates to the first norm described above. That is, the stray current activity should be dependent on the solar irradiation profile. As clearly illustrated, the operation of a PV plant can be broadly classified in one of two different “states”. The sun is down and there is no PV production (thus no stray current activity is anticipated). The sun is up and there is - a solar irradiation dependent - PV production (thus a varying stray current activity).

For estimating the levelized seasonal values of current flow through the DC cables a statistical approach is followed. The dc current measurements obtained over a complete year are statistically treated to determine an empirical probability distribution that captures the variation of DC current flow through the cables in percent of their rated  $I_{sc}$ . The statistical analysis should reflect only on the dc current measurements obtained during the operating/ generating hours of the PV system over a year. To this extent, Fig. 10 shows the empirical probability distribution (of each season) that describes the variation of DC current values (in percent of cables’ rated  $I_{sc}$ ) flow through DC cables. Taking the probability distribution of summer as an example, one can extract that a current flow of approximately 55% of the cables’ rated  $I_{sc}$  can occur at 11% probability.

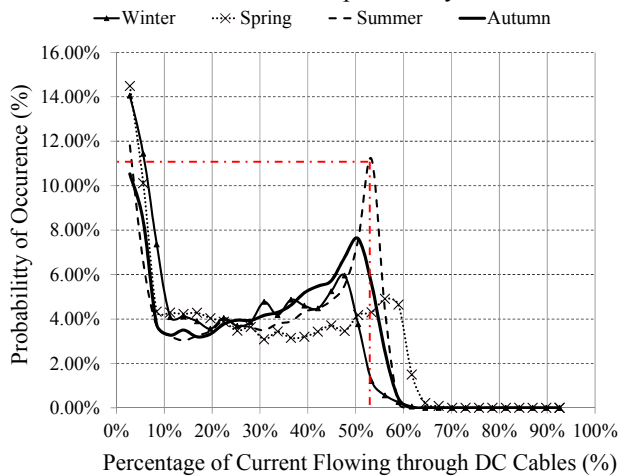


Fig. 10. Seasonal Probability Distributions showing DC current values (in percent of cables’ rated  $I_{sc}$ ) flow through DC cables.

The empirical distribution probabilities are subsequently used to obtain a levelized value of the current flowing through the DC cables in each of the four seasons (winter, spring, summer and autumn) during the operating hours of the PV system. Then, as dictated by the second norm above, each season should be assigned to a representative soil resistivity, since the latter will also impact on the level of stray current flowing through the soil.

Therefore, Table IV shows the evaluated levelized current values (%) flowing through the DC cables (using the statistical distributions displayed in Fig.10) and an assumed representative soil resistivity value for each of the four seasons.

TABLE IV  
REPRESENTATIVE SEASONAL DC CURRENT VALUES AND SOIL RESISTIVITIES

	Levelized Current Values (% of rated $I_{sc}$ )	Soil Resistivity ( $SR$ ) ( $\Omega.m$ )
Winter	33.57%	$SR \sim 10 \Omega.m$
Spring	38.44 %	$10 \Omega.m < SR < 100 \Omega.m$
Summer	43.34 %	$SR \geq 100 \Omega.m$
Autumn	41.51%	$10 \Omega.m < SR < 100 \Omega.m$

## 2) Calculation of Annual Corrosion Impact

The general assumptions and statistical treatment of the PV generation data can be used to estimate the metal loss arising from the corresponding stray current leakage. As a first step, the derived percentages in Table IV can be used as benchmark. This is because they empirically capture the stochastic nature of PV generation derived from historical data. These are utilized to subsequently determine the varying levels of stray currents leaving the DC cables over a future evaluation period. To this end, the percent seasonal levelized currents shown in Table IV are tailored to the characteristics of the physical model considered in this paper (Section III - A). The corresponding absolute current values are shown in Table V.

TABLE V  
WEIGHTED AVERAGE DC CURRENT VALUES FLOWING THROUGH THE CABLES

	Weighted Average Current Values	
	For DC Cables Leading to the Central Combiner	For DC Cables Leading to the Central Inverter
Winter (33.57%)	47.86 A	287.14 A
Spring (38.44%)	54.80 A	328.84 A
Summer (43.34%)	61.79 A	370.73 A
Autumn (41.51%)	59.18 A	355.10 A

Therefore, four static models are formulated, one for each season. The simulation principles and data of these models are identical to the process described in Section V – A and Table I, albeit: a) adjusting for the energisation currents of each DC cable using the absolute current values of Table V and b) adjusting for the soil resistivity value of each season (Table IV). In the interest of space, Fig. 11 only shows snapshots of the corrosive stray current for the metallic pipeline (Fig. 4), for each season.

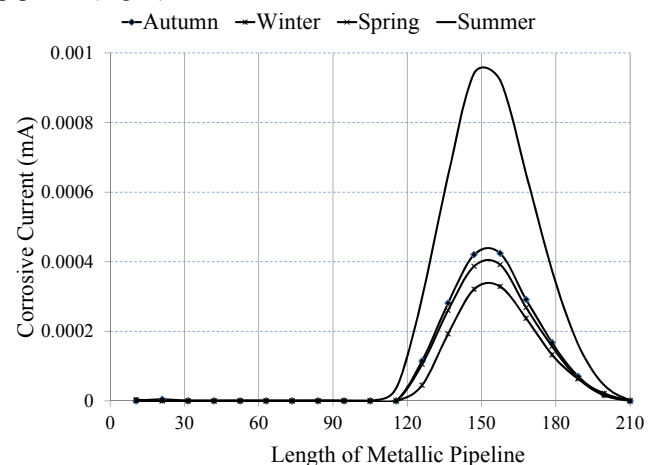


Fig. 11. Snapshots of Corrosive Leakage Current for Each Season– for the specific system modelled

The corrosive stray current is defined as the current leaking from a conductor to an electrolyte i.e. the positive values of leakage current. These results should be appropriately post-processed to estimate the cumulative mass of metal lost by electrolysis. Within this paper, the metal lost is calculated for the copper grounding electrodes and the lead (Pb) coating layer of the metallic pipeline (see Table I). The post processing procedure is described below.

For each season, a static leveled profile of the corrosive leakage current along the length of the buried metallic infrastructure (Fig. 11) is produced. It is therefore assumed that this leveled profile will apply for every second of the PV operating hours, within each season. This assumption is necessary to crudely estimate the corrosive leakage charge ( $Q_L$ ) that would be accumulated on the metallic infrastructure in each season. Thus, under the Faraday's law, the mass of metal produced by electrolysis would be proportional to the quantity of charge accumulated ( $Q_L$ ). The calculation rationale is provided in (1).

$$n(e^-) = \frac{Q_L}{F} \rightarrow MML = MM \times n(e^-) \quad (1)$$

Where  $n(e^-)$  is the moles of deposited metal,  $Q_L$  is the corrosive leakage charge accumulated over the season,  $F$  is the Faraday's constant ( $96484 \text{ C.mol}^{-1}$ ),  $MML$  is the mass of metal lost in g and  $MM$  is the molar mass of metal in  $\text{g.mol}^{-1}$ .

The final post processing step includes the superposition of the metal lost estimated separately in each season. This is to provide an annual estimate of the corrosion impact on the metallic infrastructure. The principle of superposition is a valid assumption since the DC leakage corrosion concept and impact can be linearly scaled [15]. Therefore, Fig. 12 illustrates the calculated annual metal loss on the grounding electrode (closer to the metallic pipe) and the annual metal loss on the nearby metallic pipe.

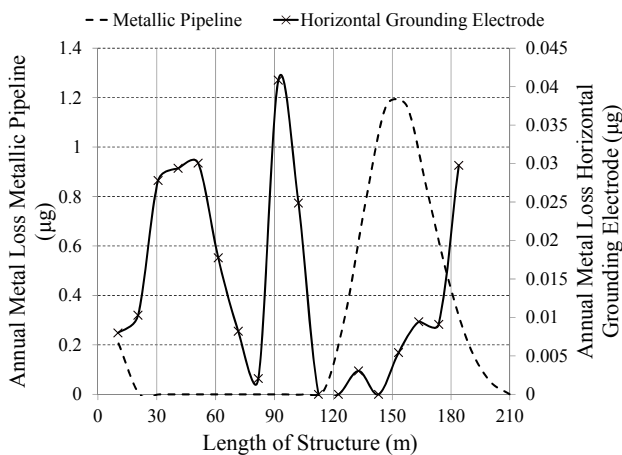


Fig. 12. Annual Metal Loss as a consequence of Stray Current Corrosion – for the specific system modelled

The metal loss calculated assumes that the corrosion damage is caused by stray current only and not by natural effects such as loss of metal passivation due to chloride ingress etc. At a macroscopic level these distributions can identify areas of conductors that will suffer lower lifetime

due to accelerated corrosion. This identification can be used to optimize the required level of corrosion protection in specific grounding sections of the PV plant or nearby metallic pipelines.

### 3) Sensitivity Analysis and Uncertainty

One of the dominant factors, in the corrosion impact assessment of the metallic pipeline and grounding electrodes, is the value assigned to the insulation coating of the buried DC cables. This is because the level of stray current relies on the insulation resistance to earth of these cables. To address this influence, a sensitivity analysis is performed to illustrate the variation in the calculated loss of metal values over a range of lower/deteriorated cables' insulation resistances. Using the metallic pipeline as an example (NB: the same concept can be applied for the grounding electrodes), Fig. 13 illustrates its annual metal loss by stray current corrosion under reduced cables' insulation to earth resistance values (e.g.  $1\text{M}\Omega.\text{km}$ ,  $100\text{k}\Omega.\text{km}$  and  $1\text{k}\Omega.\text{km}$ ).

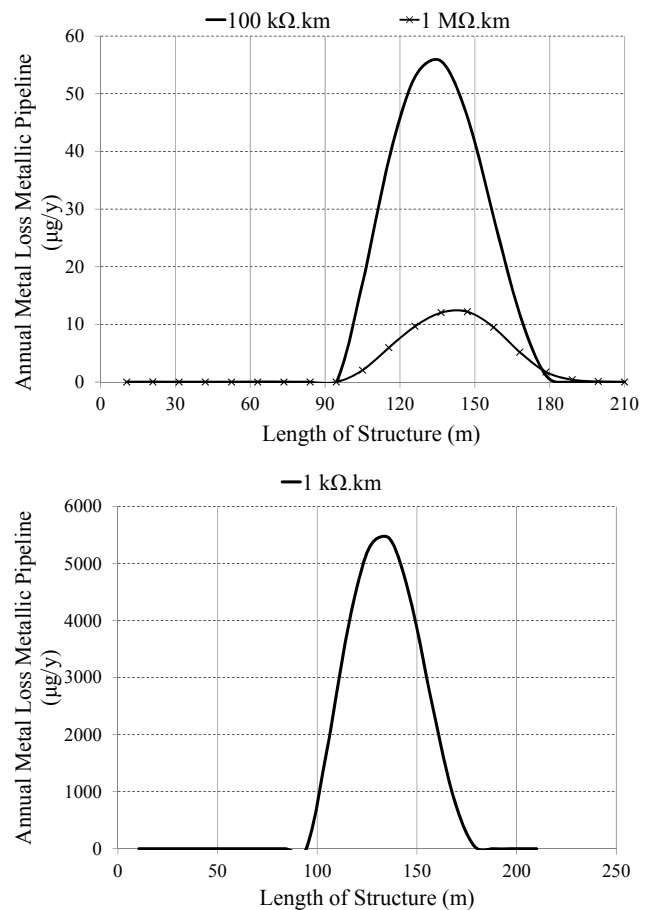


Fig. 13. Annual Metal Loss On Metallic Pipeline for Various Insulation Values of DC cables – for the specific system modelled

It should be noted that it is not unlikely for the DC cables to have deteriorated insulation with typically no loss of PV generation performance. In fact, if the corresponding leakage currents are below the detection values of the monitoring devices, then these may go unattended for a significant

amount of time. The 100 k $\Omega$ .km and 1k $\Omega$ .km values are used in the sensitivity analysis since they constitute typical industrial threshold levels. Beyond these levels an alert is raised by the inverters to cease the operation of PV plants. This is because smaller insulation resistances than the specified thresholds, can cause dangerous leakage currents.

Hence, the results in Fig. 13 can be benchmarked against the results shown in Fig. 12. It is clear that under deteriorated insulation conditions, the metal lost by corrosion significantly increases. For example, at 1k $\Omega$ .km cables' insulation resistance the maximum value of metal lost by corrosion along the length of the metallic pipeline is 5500  $\mu$ g/y whereas at 26.23 M $\Omega$ .km (Table I) the maximum value of metal lost is 1.2  $\mu$ g/y (Fig.12).

Moreover, it should be noted that of all the parameters detailed in this study, the soil resistivity is likely to introduce the greatest source of uncertainty into the modeling process. The soil resistivity (and structure) is, however, difficult to capture and will change as a function of the seasons/weather conditions. The work reported in [16], [17] states that: a) soil-resistivity measurements can be in error by as much as 50% when measurements are taken in proximity to metallic buried structures and b) soil resistivities can change in a local environment by a factor of 20 according to the level of moisture present with a soil.

To this end, under the parameters described (Table I) and the model developed (Fig. 4), an uncertainty in the assumed soil resistivity value in the order of 20% for example, will provide a disparate uncertainty in the calculated metal loss (shown in Figs 12 and 13) in the order of 13%.

Finally, it should be also appreciated that DC leakage currents would significantly increase in the event of DC ground faults, however the impact of these faults on the metal lost, will be heavily dependent on the magnitude of fault and its duration.

## VI. INTERPRETATION AND CONCLUDING REMARKS

A holistic top-down approach to assess the impact of stray current corrosion resulting from the operation of a relatively large solar plant is provided. The approach followed integrates the intrinsic characteristics of photovoltaic current generation and the accurate topological arrangement of some important metallic infrastructure likely to be present in or near a PV plant. The approach followed also integrates the soil and material characteristics associated with the PV plant's infrastructure.

Calculation of metal loss arising from stray current corrosion is determined from Faraday's laws, which for steel give a relationship that 1 amp.year of current will corrode approximately 9.1kg or 33 kg of lead. Within this paper, the absolute values of the metal loss calculated should be interpreted with care, as these are quite dependent on the specifics of the PV plant considered in the analysis. However, the impact of stray current corrosion is thoroughly assessed in DC traction systems [18] and a fair analogy on its consequences can be drawn when assessing the impact resulting from the operational principles of large solar plants. To this end, it is highlighted that the stray current picture in

large solar systems is heavily dominated by the insulation condition of underground DC cables, the size and age of the PV plant as well as the soil characteristics (e.g. moisture content) of the area it occupies. This clearly suggests that the extent of stray current corrosion would be specific to the characteristics and topology of each installation. However, the general conclusion that can be extracted is that, under certain conditions, DC stray corrosion may exist in large scale PV applications.

Therefore, as a conclusive message, we wish to highlight that DC stray corrosion impact has forced stakeholders across the world to impinge a variety of design specifications, codes of practice and international standards [18], [19] mainly for DC traction project designs. Such codes and standards are intended to provide designers and utility companies with a corrosion management strategy that defines a level of corrosion risk which is acceptable across infrastructures. The development of similar corrosion management systems and practices may be necessary for PV plant owners and Distribution Network Owners. One should also note that a typical useful life-cycle of commercial PV systems is around 25 years. Thus, system designers and contractors should ensure a similar life-cycle for the grounding and supporting/foundation infrastructure of these systems and at the same time provide evidence that every effort is pursued to prevent damage to third-party utility services routed in areas near PV plants.

## REFERENCES

- [1] Dugan, R.C.; McDermott, T.E., "Distributed generation," *Industry Applications Magazine*, IEEE , vol.8, no.2, pp.19,25, Mar/Apr 2002 doi: 10.1109/2943.985677
- [2] Simoes, M.G.; Roche, R.; Kyriakides, E.; Suryanarayanan, S.; Blunier, B.; McBee, K.D.; Nguyen, P.H.; Ribeiro, P.F.; Miraoui, A., "A Comparison of Smart Grid Technologies and Progresses in Europe and the U.S.," *Industry Applications*, IEEE Transactions on , vol.48, no.4, pp.1154,1162, July-Aug. 2012 doi: 10.1109/TIA.2012.2199730.
- [3] D. H. McIntosh, "Grounding where corrosion protection is required," *Industry Applications*, IEEE Transactions, vol. IA-18, no. 6, pp. 600-607, 1982.
- [4] S. Rajan and S. I. Venugopalan, "Corrosion and grounding systems," *Industry Applications*, IEEE on, vol. IA-13, no. 4, pp. 297-306, 1977.
- [5] Parise, G.; Parise, L.; Martirano, L.; Farber, A.; Katz, B., "Grounding System Adequacy of HV/MV Substations in Areas with Reduced Accessibility" *Industry Applications*, IEEE Transactions on , vol.PP, no.99, pp.1,1,doi: 10.1109/TIA.2014.2379952
- [6] Lopez, O.; Freijedo, F.D.; Yepes, A.G.; Fernandez-Comesaa, P.; Malvar, J.; Teodorescu, R.; Doval-Gandoy, J., "Eliminating Ground Current in a Transformerless Photovoltaic Application," *Energy Conversion*, IEEE Transactions on , vol.25, no.1, pp.140,147, March 2010 doi: 10.1109/TEC.2009.2037810.
- [7] IEC-50539-11-2010: "Low-voltage surge protective devices surge protective devices for specific application including d.c. Part 11 requirements and tests for spds in photovoltaic applications.
- [8] J. Gorman, M. Arey, and G. Koch, "Cost of corrosion in the electric power industry," *Electric Power Research Institute*, Rep. 2001.
- [9] C. A. Charalambous, N. Kokkinos, N. Christofides, "External Lightning Protection and Grounding in Large Scale Photovoltaic Applications", *Electromagnetic Compatibility*, IEEE Transactions on, vol.56, no.2, pp.427,434, April 2014.
- [10] IEC- 62446: 2009 - Grid connected photovoltaic systems - Minimum requirements for system documentation, commissioning tests and inspection, clause 5.4.7.2, 2009.

- [11] I. Cotton, C. Charalambous, P. Ernst, P. Aylott, "Stray Current Control in DC Mass Transit Systems", IEEE Transactions on Vehicular Technology, Vol. 54, No. 2, pages: 722 – 730, March 2005.
- [12] CDEGS Software, Safe Engineering Services & Technologies Ltd Montreal, Quebec, Canada Est. 1978.
- [13] Dawalibi, F.P.; Ma, J.; Southey, R.D.; , "Behaviour of grounding systems in multilayer soils: a parametric analysis," Power Delivery, IEEE Transactions on , vol.9, no.1, pp.334-342, Jan 1994 doi: 10.1109/61.277704.
- [14] University of Cyprus Photovoltaic Technology at <http://www.pvtechnology.ucy.ac.cy/pvtechnology/>, accessed December 2014.
- [15] C.A. Charalambous and Aylott, P., "Dynamic Stray Current Evaluations on Cut-and-Cover Sections of DC Metro Systems", Vehicular Technology, IEEE Transactions on, vol.63, no.8, pp.3530, 3538, Oct. 2014.
- [16] Ma, J., and Dawalibi, F.P.: 'Study of influence of buried metallic structures on soil resistivity measurements', Power Delivery, IEEE Transactions on,1998, 13, (2), pp. 356–365
- [17] He, J., Zeng, R., Gao, Y., Tu, Y., Sun, W., Zou, J., and Guan, Z.: 'Seasonal influences on safety of substation grounding system', Power Delivery, IEEE Transactions on, 2003, 18, (3), pp. 788–795
- [18] EN-50162-2004; 'Protection against corrosion by stray current from direct current systems' August 2004.
- [19] EN 50122-2: "Railway Applications – Fixed Installations – Electrical Safety, earthing and the return circuit – Part 2: Provisions against the effect of stray currents caused by d.c. traction systems", October 2010.

## BIOGRAPHIES

**Charalambos A. Charalambous** received a Class I BEng (Hons) degree in Electrical & Electronic Engineering in 2002 and a PhD in Electrical Power Engineering in 2005 from UMIST, UK (The University of Manchester). He was with the High Voltage Lab of the University of Manchester from 2005-2009. As of 2010, he is an Assistant Professor, in the Department of Electrical and Computer Engineering, at the University of Cyprus. He is the director of the Power System Modelling Laboratory that operates under the auspices of FOSS Research Centre of Sustainable Energy. His current research interests include solar applications, DC induced corrosion and control in power system application, earthing/grounding and life-cycle losses evaluations of transformers.

**Andreas Demetriou** received a MEng (Hons) degree in Electrical & Computer Engineering in 2013 National Technical of Athens (NTUA). He is a research assistant within the Power System Modelling Laboratory that operates under the auspices of FOSS Research Centre of Sustainable Energy, University of Cyprus. His current research interests include grounding and lightning protection of large scale solar applications.

**Nikolaos D. Kokkinos** received the M.Sc and Ph.D. degrees in High Voltage Engineering from UMIST in 2001 and 2004 respectively. He is now the technical manager of the research and development department of ELEMKO, SA. Since 2007, he is an active member as an expert in 1) the International standardization committee IEC SC 37A, 2) in the European standardization committee CLC TC 37, and 3) in the European standardization committee CLC SC 9XC.